

Research Article

Particle Size Effects of TiO₂ Layers on the Solar Efficiency of Dye-Sensitized Solar Cells

Ming-Jer Jeng,¹ Yi-Lun Wung,¹ Liann-Be Chang,¹ and Lee Chow²

¹ Department of Electronic Engineering and Green Technology Research Center, Chang-Gung University, Taoyuan 333, Taiwan

² Department of Physics, University of Central Florida, Orlando, FL 32816, USA

Correspondence should be addressed to Ming-Jer Jeng; mjjeng@mail.cgu.edu.tw

Received 11 October 2012; Accepted 22 March 2013

Academic Editor: Tianxin Wei

Copyright © 2013 Ming-Jer Jeng et al. This is an open access article distributed under the Creative Commons Attribution License, which permits unrestricted use, distribution, and reproduction in any medium, provided the original work is properly cited.

Large particle sizes having a strong light scattering lead to a significantly decreased surface area and small particle sizes having large surface area lack light-scattering effect. How to combine large and small particle sizes together is an interesting work for achieving higher solar efficiency. In this work, we investigate the solar performance influence of the dye-sensitized solar cells (DSSCs) by the multiple titanium oxide (TiO₂) layers with different particle sizes. It was found that the optimal TiO₂ thickness depends on the particle sizes of TiO₂ layers for achieving the maximum efficiency. The solar efficiency of DSSCs prepared by triple TiO₂ layers with different particle sizes is higher than that by double TiO₂ layers for the same TiO₂ thickness. The choice of particle size in the bottom layer is more important than that in the top layer for achieving higher solar efficiency. The choice of the particle sizes in the middle layer depends on the particle sizes in the bottom and top layers. The mixing of the particle sizes in the middle layer is a good choice for achieving higher solar efficiency.

1. Introduction

Dye-sensitized solar cells (DSSCs) have attracted much attention as good candidates for low-cost, good-stability, and high-efficiency solar cells [1, 2]. There are many innovations in this emerging technology like the new dyes which absorb a longer range of wavelengths and the proposed nanostructure titanium oxides (TiO₂) for increasing surface area and so forth [3–6]. The DSSCs with the nanostructure titanium oxide/porphyrins dye thin films on TCO glass can achieve a solar efficiency as high as with 13% [7]. The major improvement of the research is not only by introducing artificial synthesized dye as light harvesters instead of TiO₂ itself, but also by using the nanostructure layer to improve the absorption and collection efficiency. In principle, rapid electron transport and slow recombination will be better for obtaining high solar conversion efficiency. For conventional DSSCs, the mesoporous photoelectrode films composed of small-sized TiO₂ nanocrystalline particles have the advantages of providing a large surface for greater dye adsorption and facilitating electrolyte diffusion within their pores [8]. Therefore, optimizing the microstructure of the photoanode is vital for

developing high solar efficiency of DSSCs. Recently, the light-scattering effects of TiO₂ electrode have been proposed by using different particles in the TiO₂ layers, which can significantly improve the light harvest efficiency [9]. Ferber and Luther [10] and Rothenberger et al. [11] confirmed the light-scattering effect with the transport theory and the many-flux model, respectively. Except for the scattering abilities of TiO₂ layers, it is also important that the TiO₂ electrode has a larger surface area, which can increase the dye adsorption and then high photocurrent generation. Recently, many efforts have been focused on the development of multifunctional TiO₂ nanostructures for application in the DSSCs [12–19]. However, they lack a systematic study for particle size effects. It is known that the large particle size of TiO₂ layers can result in a strong light scattering ability and increase an optical absorption path. It indicates that it has higher short circuit current. However, the small nanoparticle size of TiO₂ layers has large contact area and low contact resistance. It means that it has higher open circuit voltage. How to combine large and small nanoparticle sizes together is an interesting work for achieving higher solar efficiency. In this work, we investigate the performance influence of DSSCs

prepared by multiple TiO₂ layers with different particle sizes systematically.

2. Experiments

The 2 cm × 1.5 cm fluorine-doped SnO₂ (FTO) electrodes (sheet resistance 8 Ω/square) were cleaned by acetone, isopropanol, and deionized water sequentially. TiO₂ solutions are prepared by mixing 3 g of TiO₂ powders with different particle sizes, 1 mL of TTIA, 0.5 g of polyethylene glycol (PEG), and 0.5 mL of Triton X-100 in 50 mL of isopropanol (IPA), and then ground and stirred by zirconia ball for 8 hours. It is known that the addition of TTIP in the solution can reduce the surface crack and that the PEG can make a porous thin film by annealing. The TiO₂ thin films were formed by spin-coating TiO₂ solutions on FTO glass and annealed at 500°C for one hour. Three structures of single, double, and triple TiO₂ layers with different particle sizes were prepared. The commercial TiO₂ powders with different particle sizes used in the experiments are listed in Table 1. For double or triple layers, their total thicknesses are controlled to be the same of 12 μm (not an optimal thickness). It is noted that the thickness of each layer of TiO₂ film can influence the results of solar performance parameters and EIS of DSSCs. We did our best to control the thickness of each layer of TiO₂ film to be about 6 and 4 μm, respectively, for double and triple layers. TiO₂ photoelectrodes were immersed for 24 hrs in anhydrous ethanol solution containing 3 × 10⁻⁴ M N719 dye. The liquid electrolyte consisted of 1 M lithium iodide (LiI), 0.1 M iodine (I₂), 0.5 M 4-tert-butylpyridine (TBP), and 0.6 M 1,2-dimethyl-3-propylimidazolium iodide (DMPII) in acetonitrile. The cathode electrode was made by FTO, which is coated by H₂PtCl₆ precursor and annealed at 450°C for 30 min. The cell was fabricated by applying Surlyn, with a thickness of 60 μm between the two electrodes, and the gap was fixed at 60 μm. Two FTO glasses were made with the Surlyn heated at 100°C. The electrolyte was injected into the space between the electrodes by capillarity. Finally, these two FTO glasses were sealed completely. The active area of cells is 0.25 cm². The photocurrent-voltage (I-V) characteristic curves were measured by Keithley 2420 under AM1.5G illumination. Light absorption was measured by a UV-vis spectrophotometer. In addition, electrochemical impedance spectroscopy (EIS) is used to analyze the charge transport resistance [20–24].

3. Results and Discussion

The strong back-scattering light due to the large particles near the conducting glass unavoidably results in a light loss. To reduce light loss due to the strong back-scattering light, multiple-layer structure of TiO₂ has been proposed to deposit the small particles first on the conducting glass for increasing contact area and then followed by the large particle layers for back-light scattering. To examine the particle size effect on the solar performance of DSSCs systemically, three structures of single, double, and triple TiO₂ layers with different particle sizes are investigated. For single TiO₂ layer, different particle sizes and thicknesses of TiO₂ are studied. Different particle

TABLE 1: The commercial TiO₂ particle sizes used in the experiments.

TiO ₂ powder	Average particle sizes (nm)		
Small particles	5	9 or 10	
Medium particles	21	40	
Large particles	100	200	400

sizes in the top, middle, and bottom layers are examined, respectively, for the double or triple TiO₂ layers.

Figure 1 shows the cross section and surface-view field emission scanning electron microscopy (FESEM) images of single TiO₂ layer with three different particle sizes of 21 nm, 100 nm, and 200 nm. The solar efficiency dependence on the thickness of TiO₂ layer with different particle sizes is shown in Figure 2. Clearly, the DSSCs with the large particle size of TiO₂ layer have lower solar efficiency than those with small particle size of TiO₂ layer under the same TiO₂ thickness. The lower solar efficiency in large particle sizes of TiO₂ layer can be attributed to a strong back-scattering light and can result in lower solar efficiency. It is known that the large particle size of TiO₂ layer has smaller surface area than the small one. The number of adsorbed dyes in large particle size of TiO₂ layer is less than that in small particle size of TiO₂ layer due to small surface area. Therefore, the photocurrent of the DSSCs with large particle size of TiO₂ layer is smaller than that with small particle size of TiO₂ layer and results in lower solar efficiency. It is also observed that the optimal TiO₂ thickness depends on the particle sizes of TiO₂ layer for achieving the maximum efficiency. The larger the particle sizes of TiO₂ layers, the shorter the optimal TiO₂ thickness due to a strong back-scattering light. The larger thickness of TiO₂ layers is expected to adsorb more dyes. But the generated electron in dyes cannot be injected to electrode effectively due to long distance when the thickness of TiO₂ layers is long enough. Thus, the optimal thickness of TiO₂ layers is different for each particle size due to different back-scattering lights and charge transport properties in the DSSCs. Dyes in the TiO₂ layers will build up with increasing thickness and hence increase the photocurrent. However, thicker TiO₂ layers will result in a decrease in the transmittance of TiO₂ layers and thus reduce the incident light intensity to dyes. In addition, the charge transfer resistance increases with the increasing thickness of TiO₂ layers. The charge recombination between electrons injected from the excited dye to the conduction band of TiO₂ and the I₃⁻ ions in the electrolyte will become more serious in thicker TiO₂ layers.

Figure 3 shows the schematic diagrams of double-layer structures with the different particle sizes in the top and bottom layers. The cross section FESEM images of double TiO₂ layers with (a) 400 nm/5 nm/FTO, (b) 400 nm/100 nm/FTO, (c) 400 nm/200 nm/FTO, (d) 100 nm/10 nm/FTO, (e) 200 nm/10 nm/FTO, and (f) 400 nm/10 nm/FTO are shown in Figure 4. It is clear to demonstrate the different particle sizes in the top and bottom layers. Figures 5(a) and 5(b) show the photocurrent-voltage curves of the DSSCs with double-layer structures of different TiO₂ particle sizes in the bottom and top layers, respectively. Clearly, the DSSCs

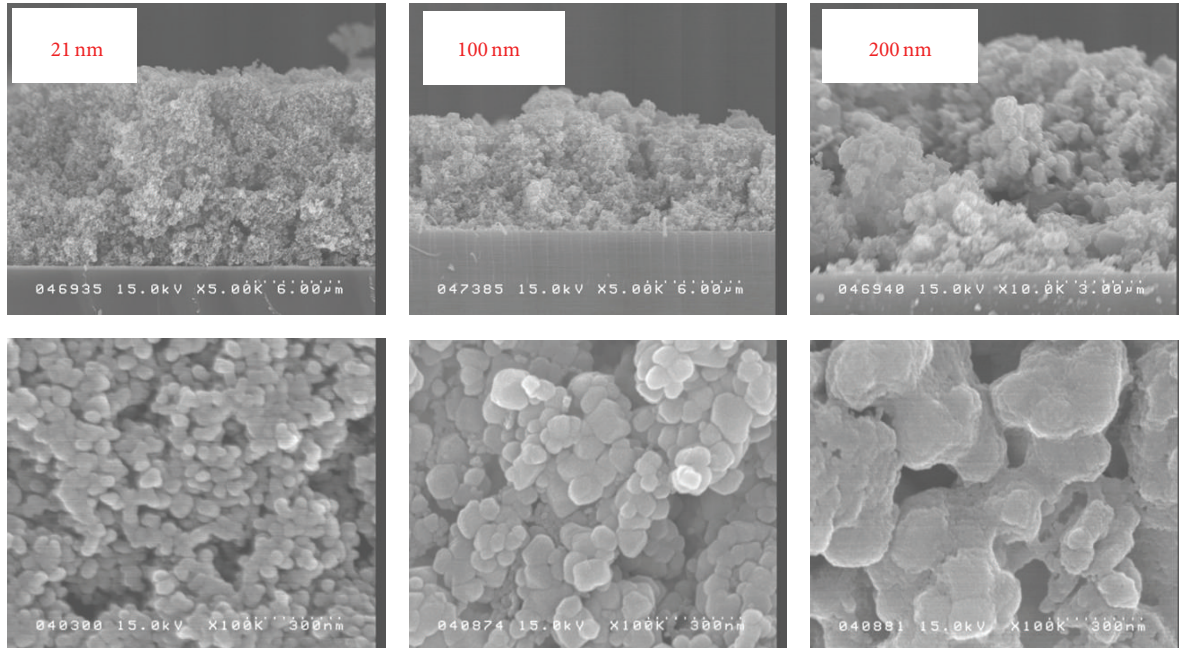


FIGURE 1: The cross section and surface-view field emission scanning electron microscopy (FESEM) images of a single TiO_2 layer with three different particle sizes of 21 nm, 100 nm, and 200 nm.

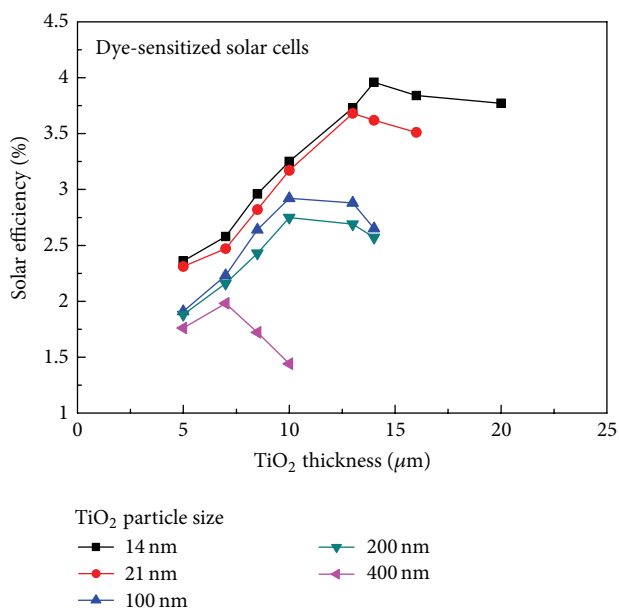


FIGURE 2: The solar efficiency dependence on the thickness of TiO_2 layers with different particle sizes.

with smaller particle size of 5 nm in the bottom have larger short-circuit current and efficiency than those with larger particle sizes of 100 and 200 nm, as shown in Figure 5(a). It is known that smaller particles of TiO_2 layers have large surface areas and adsorb more dyes. Hence, they have low contact resistance and high photocurrent. In addition, the strong back-scattering light due to large particle size of 400 nm

will also increase the reabsorption in the small particle size of TiO_2 layer. These smaller particle sizes in the bottom are beneficial to recapture the scattering light from the top scattering layer. The larger particle sizes of TiO_2 layers in the top can enhance the back-scattering light effectively and result in higher photocurrent, as shown in Figure 5(b). Thus, the combination of larger particle sizes of TiO_2 in the top and smaller particle sizes of TiO_2 in the bottom will be better for achieving higher solar efficiency. The solar performance parameters of the DSSCs with double-layer structure of different TiO_2 particle sizes in the bottom and top layers are listed in Table 2. Interestingly, the solar efficiency of DSSCs with 400 nm/10 nm/FTO, 200 nm/10 nm/FTO, or 100 nm/10 nm/FTO structure is much higher than that with 400 nm/100 nm/FTO or 400 nm/200 nm/FTO structure. It means that the choice of particle size in the bottom layer is more important than that in the top layer for achieving higher solar efficiency. Figures 6(a) and 6(b) show the light absorption of double-layer structures with different TiO_2 particle sizes in the bottom and top layers, respectively. The TiO_2 layers with smaller particle sizes in the bottom exhibit higher light absorption than those with larger particle sizes, as can be seen in Figure 6(a). The TiO_2 layers with larger particle sizes on the top layer exhibit higher light absorption than those with smaller particle sizes, as can be seen in Figure 6(b) [25]. The absorption behaviors in Figures 6(a) and 6(b) are consistent with the observation of photocurrent in Figures 5(a) and 5(b), respectively.

To study the charge transfer effects, electrochemical impedance spectroscopy (EIS) is a useful method for analysis of charge transport process [20–24]. The schematic diagram of the internal resistance related to the charge transfer kinetics

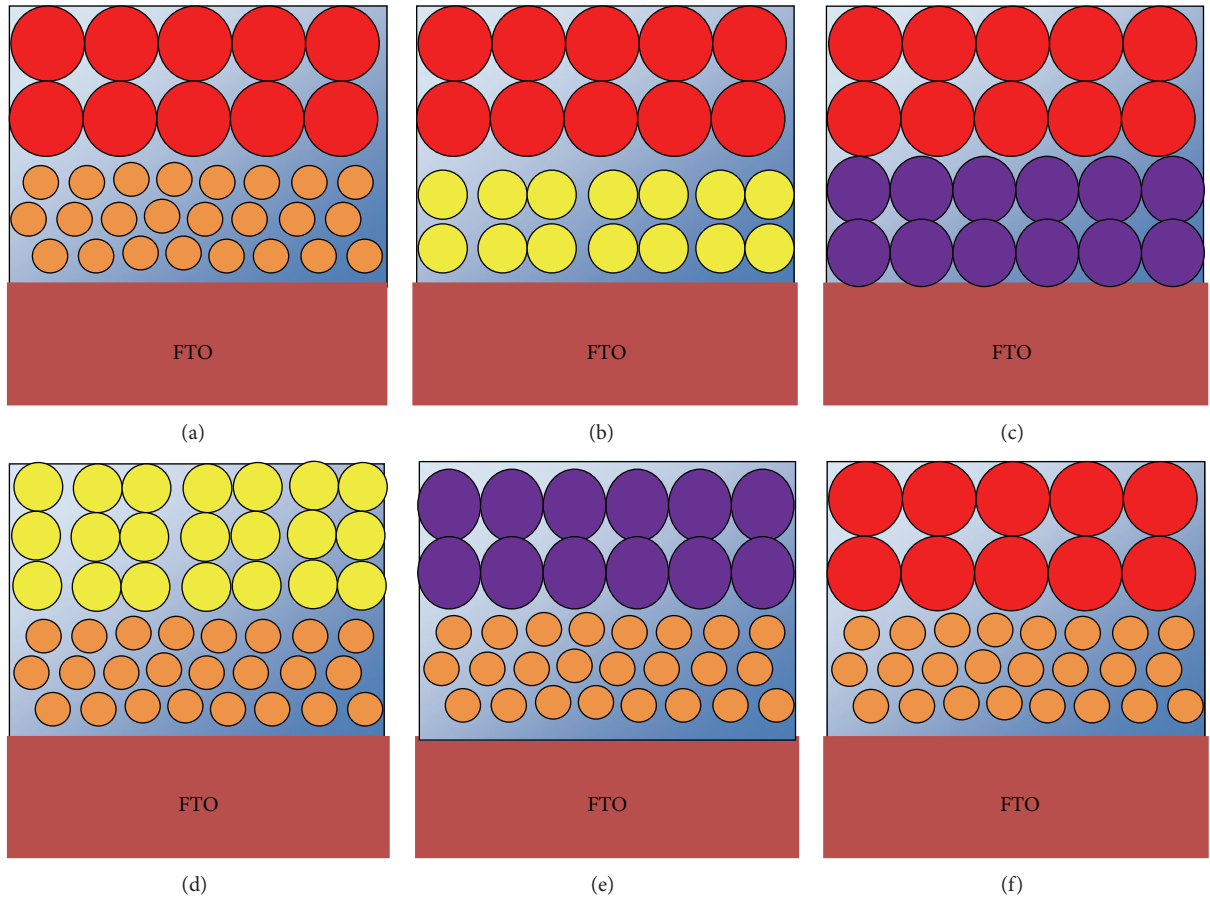


FIGURE 3: The schematic diagrams of double-layer structures with the different particle sizes in the top and bottom layers.

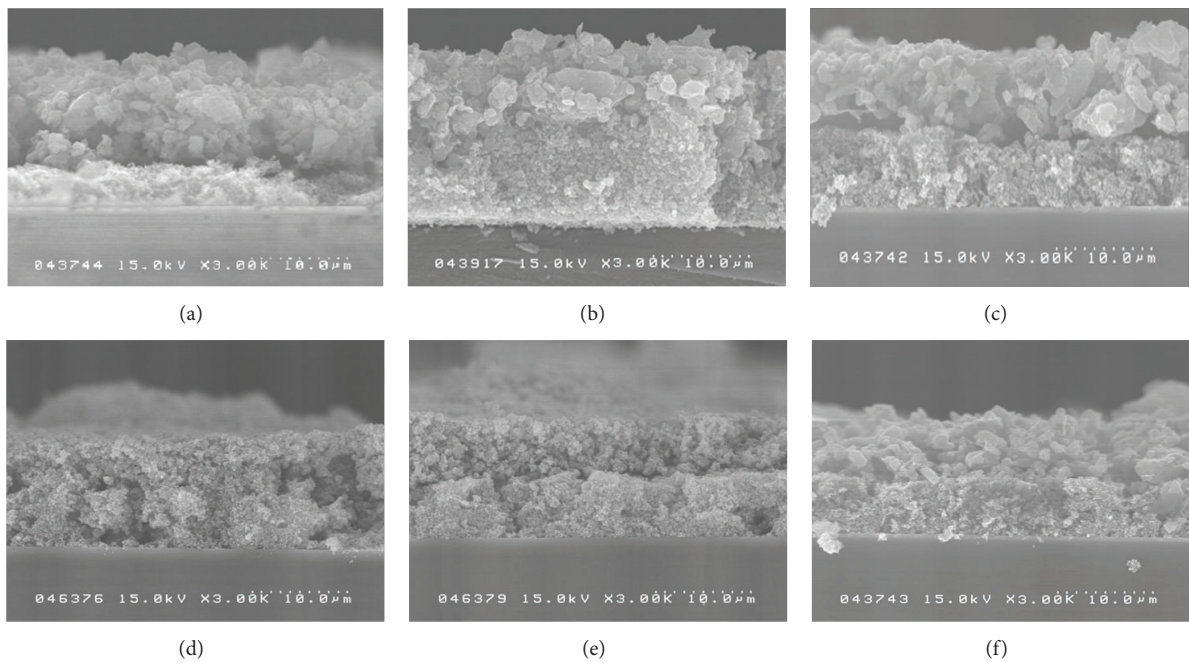


FIGURE 4: The cross section FESEM images of double TiO_2 layers with (a) 400 nm/5 nm/FTO, (b) 400 nm/100 nm/FTO, (c) 400 nm/200 nm/FTO, (d) 100 nm/10 nm/FTO, (e) 200 nm/10 nm/FTO, and (f) 400 nm/10 nm/FTO.

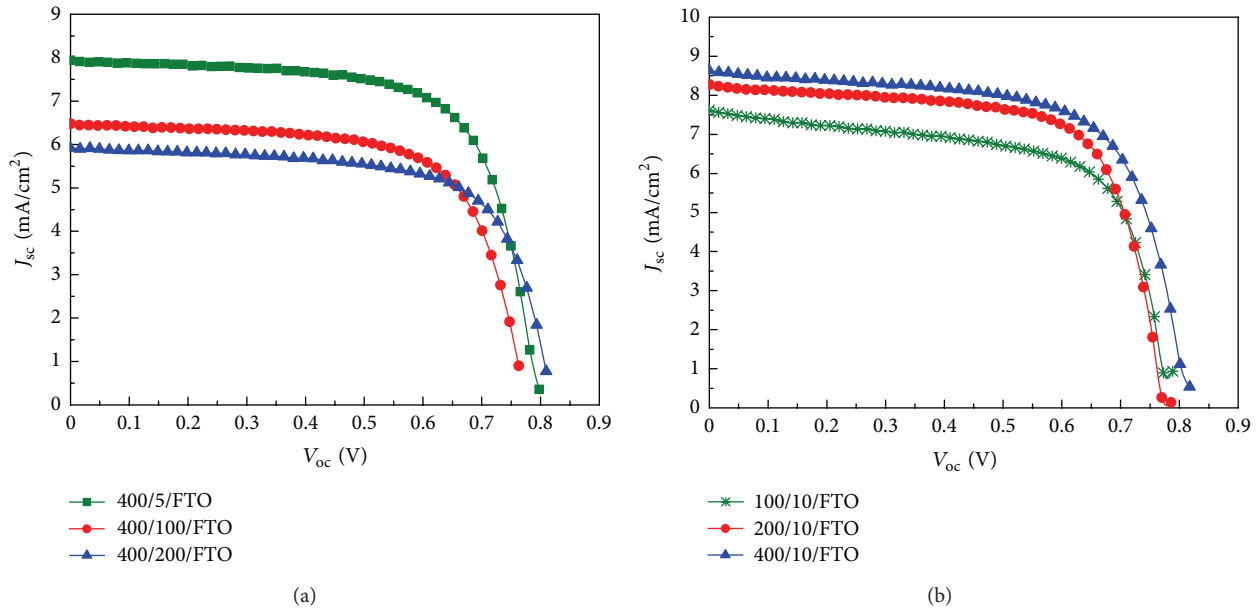


FIGURE 5: The photocurrent-voltage curves of DSSCs with double-layer structures of different TiO_2 particle sizes in the (a) bottom and (b) top layers, respectively.

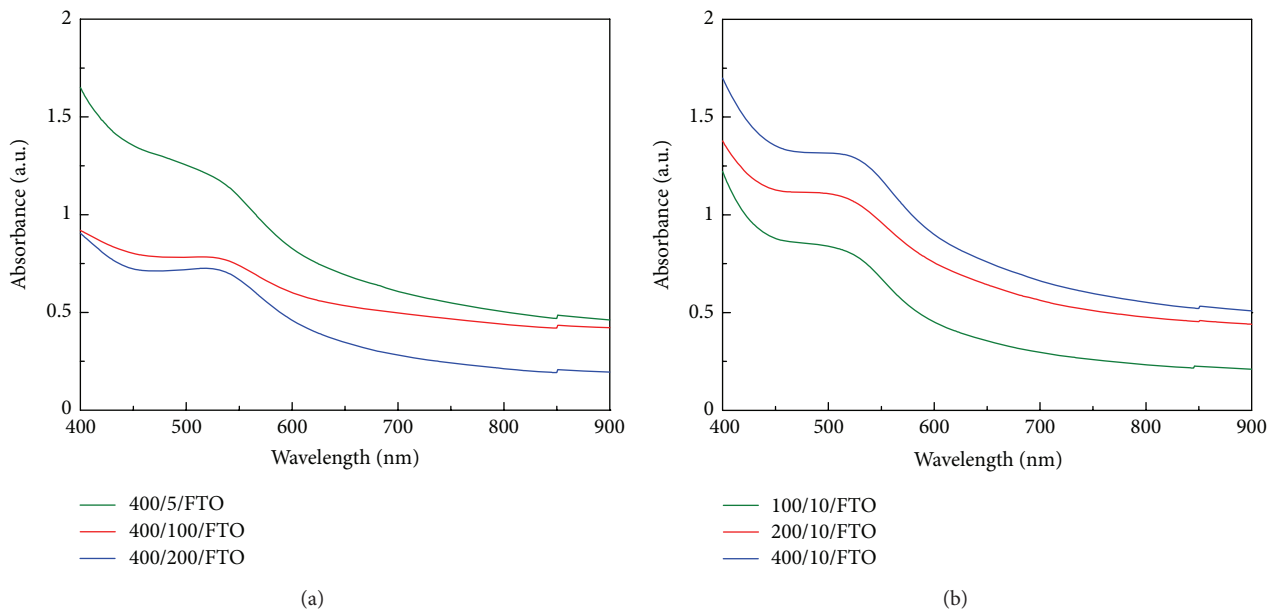


FIGURE 6: The light absorption of double-layer structures with different TiO_2 particle sizes in the (a) bottom and (b) top layers, respectively.

in the DSSCs is shown in Figure 7. In general, the Nyquist plots exhibit three semicircles. The three semicircles are attributed to the redox reaction at the platinum counter electrode (Z1) in the high-frequency region, the electron transfer at the $\text{TiO}_2/\text{dye}/\text{electrolyte}$ interface (Z2) in the middle-frequency region, and carrier transport by ions within the electrolytes (Z3) in the low-frequency region. The resistance elements R1, R2, and R3 are described as the real parts of Z1, Z2, and Z3, respectively [26]. Figures 8(a) and 8(b) show the EIS curves of the DSSCs prepared by double-layer structures

with different TiO_2 particle sizes in the bottom and top, respectively, in the form of the Nyquist plots. Two semicircles are observed in these two figures. The semicircle at low-frequency region merged with the semicircle at the middle-frequency region due to the weak resistance of ions transport in the electrolytes. The charge transfer resistance of the large semicircle in the middle-frequency region may include the extent of electron transport in the photoanode [27]. It was explained that the back-transport of electrons from the FTO electrode to the I_3^- was suppressed by the introduction of

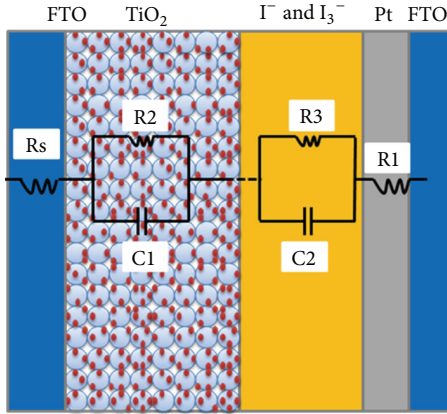


FIGURE 7: The schematic diagram of the internal resistance related to the charge transfer kinetics in the DSSCs.

small particle sizes in TiO_2 layers. During the deposition of Pt as a counter electrode, there were some slight differences such as the Pt crystallites contacting and the thickness of Pt layer between the counter electrodes. These differences caused the resistance for these two cells in the high frequency to be inconsistent [28]. The charge transport resistance parameters of EIS measurement for double TiO_2 layers are listed in Table 3. The charge transport resistance R_2 is 13.40, 18.10, and 44.33 Ω for double layers with 400/5/FTO, 400/100/FTO, and 400/200/FTO structures, respectively. The DSSCs with smaller particle size of TiO_2 layers in the bottom exhibit the lower charge transport resistance. The charge transport resistance R_2 is 18.67, 12.98, and 12.28 Ω for the double layers with 100/10/FTO, 200/10/FTO, and 400/10/FTO structures, respectively. The DSSCs with larger particle size of TiO_2 on the top exhibit the lower charge transport resistance. It is noted that the charge transport resistance in the DSSCs with 400/10/FTO structures is lower than that with 400/5/FTO structures. It means that the interface between layers with different particle sizes will be an important factor to affect the solar performance except for considering back-scattering light and surface area.

It is known that the path-depth length of light increases with wavelength. If a better solar performance is obtained, the back-scattering particles will be gradually increased. Therefore, a triple-layer structure with gradually increasing the particle size was examined. Figure 9 shows the schematic diagrams of triple-layer structures with the different particle sizes in the first (bottom), second (middle), and third (top) layers. When the light is gradually scattered with wavelength, the smaller particle underlayer will recapture the scattering light gradually from the above scattering layer. Figure 10 shows the photocurrent-voltage curves of DSSCs with triple-layer structure of TiO_2 layers. The solar performance parameters of these DSSCs are listed in Table 4. The DSSCs with 40 nm particle size in second layer exhibit higher solar efficiency than the other two of 10 and 100 nm. The fill factor degrades with the increasing particle size in the second layer due to small particle size having larger surface contact area. However, the DSSCs with 40 nm particle size in second layer

TABLE 2: Solar performance parameters of DSSCs with double-layer structure of different TiO_2 particle sizes in the bottom and top layers.

Double layers (nm)	J_{sc} (mA/cm ²)	V_{oc} (V)	Fill factor	Efficiency (%)
400/5/FTO	7.94	0.80	0.68	4.31
400/100/FTO	6.47	0.78	0.65	3.42
400/200/FTO	5.92	0.81	0.67	3.22
100/10/FTO	7.62	0.78	0.63	3.76
200/10/FTO	8.28	0.78	0.66	4.29
400/10/FTO	8.63	0.81	0.66	4.63

TABLE 3: The parameters of charge transfer resistance in double-layer structures by EIS measurements.

Double layers (nm)	R_s (Ω)	R_1 (Ω)	R_2 (Ω)
400/5/FTO	29.18	10.29	13.40
400/100/FTO	20.77	21.34	18.10
400/200/FTO	20.67	20.48	44.33
100/10/FTO	14.62	21.27	18.67
200/10/FTO	16.41	8.81	12.98
400/10/FTO	13.81	17.74	12.28

present a maximal photocurrent. It possibly indicates that if the underlayer particle wants to effectively recapture the scattering light from the above scattering layer, the particle size ratio of layer by layer should not vary too much. There exists discontinuity interface between layer and layer. This discontinuity interface cannot be neglected for multiple-layer structures. The choice of the particle sizes in the middle layer will depend on the particle sizes in the bottom and top layers. In addition, the DSSCs with larger particle sizes in the top layer exhibit higher solar efficiency due to strong back-scattering light. Figure 11 shows the photocurrent-voltage curves of DSSCs prepared by triple layers with different particle sizes and the mixing of particle sizes in TiO_2 layers. The solar performance parameters of these DSSCs are listed in Table 5. It is noted that the solar efficiency of the DSSCs in Figure 11 is higher than that in Figure 10 due to different TiO_2 thicknesses in these DSSCs. The DSSCs with smaller particle sizes of TiO_2 in the bottom layer exhibit higher solar efficiency than those with larger particle sizes of TiO_2 . The mixing of the particle sizes in the middle layers can achieve higher solar efficiency. Figure 12 shows the EIS curves of DSSCs with the triple-layer structures with different particle sizes of TiO_2 layers. The charge transport resistance parameters of EIS measurement are listed in Table 6. The DSSCs with larger particle sizes in the top layer (400 nm/200 nm/10 nm) exhibit smaller charge transfer resistance than the other two of 400 nm/100 nm/10 nm and 200 nm/100 nm/10 nm. It indicates that the choice of the particle sizes in the middle layer will affect the charge transfer resistance of TiO_2 layer. This behavior is consistent with the observation in Figure 10.

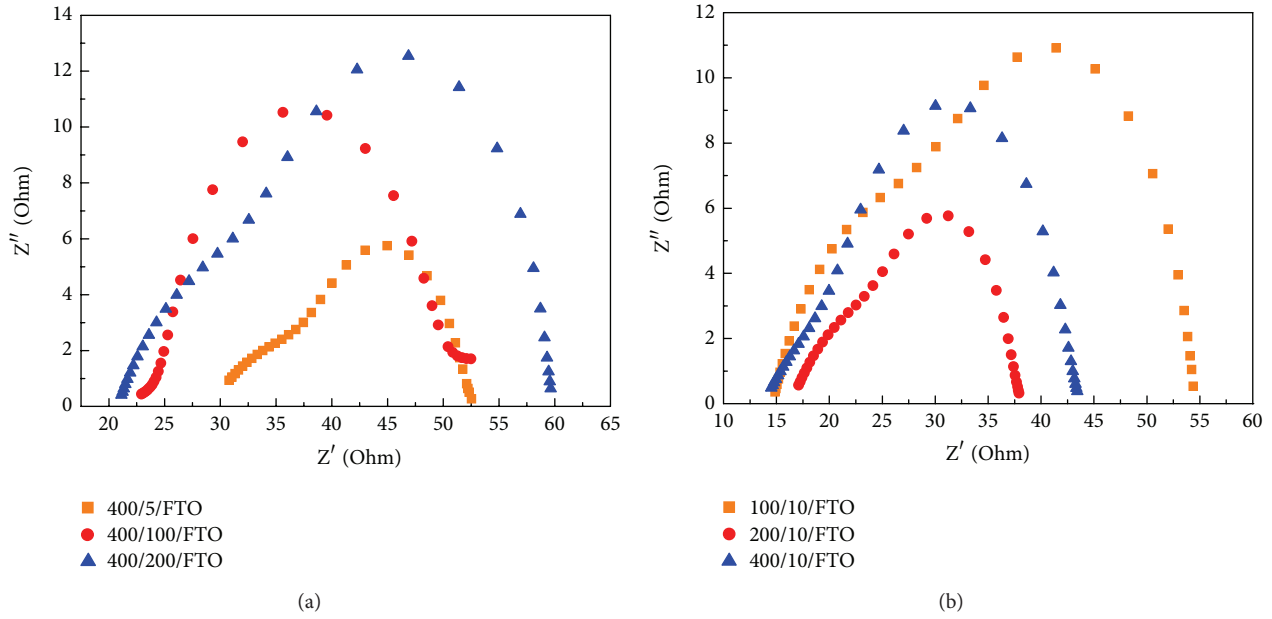


FIGURE 8: The EIS curves of the DSSCs prepared by double-layer structures with different TiO₂ particle sizes in the (a) bottom and (b) top layers, respectively, in the form of the Nyquist plots.

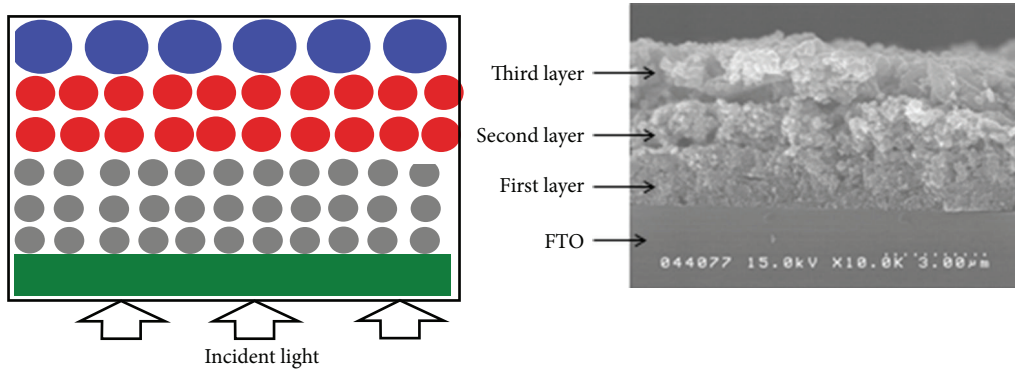


FIGURE 9: The schematic diagrams of triple-layer structures with the different particle sizes in the first (bottom), second (middle), and third (top) layers.

TABLE 4: Solar performance parameters of DSSCs with triple-layer structures of different TiO₂ particle sizes in the first (bottom), second (middle), and third (top).

Triple layers (nm)	J_{sc} (mA/cm ²)	V_{oc} (V)	Fill factor	Efficiency (%)
200/21/10	7.45	0.81	0.68	4.15
200/40/10	8.92	0.81	0.67	4.82
200/100/10	8.94	0.79	0.66	4.71
400/100/10	9.49	0.80	0.67	5.14
400/200/10	9.64	0.80	0.68	5.32

TABLE 5: Solar performance parameters of the DSSCs with triple-layer structures of different TiO₂ particle sizes in the first (bottom), second (middle), and third (top).

Triple layers (nm)	J_{sc} (mA/cm ²)	V_{oc} (V)	Fill factor	Efficiency (%)
200/100/9/FTO	10.08	0.78	0.67	5.26
200/9/100/FTO	8.46	0.77	0.65	4.28
200/9 + 100/9/FTO	10.72	0.77	0.65	5.38

4. Conclusions

The solar performance of DSSCs with different particle sizes in single, double, and triple TiO₂ layers has been investigated.

For single layer, the DSSCs with larger particle size of TiO₂ layers have lower solar efficiency than those with smaller particle size of TiO₂. The lower solar efficiency in larger particle sizes of TiO₂ can be attributed to a strong back-scattering light and less dye adsorption. In addition, the optimal TiO₂ thickness for achieving the maximum efficiency

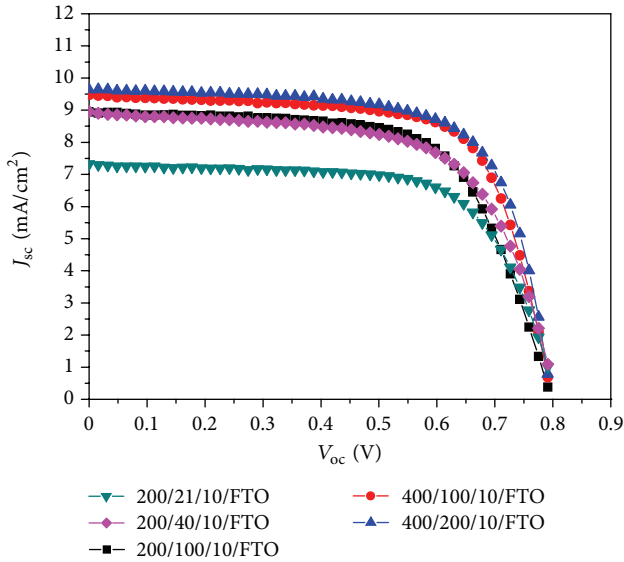


FIGURE 10: The photocurrent-voltage curves of DSSCs with triple-layer structure of TiO_2 layers.

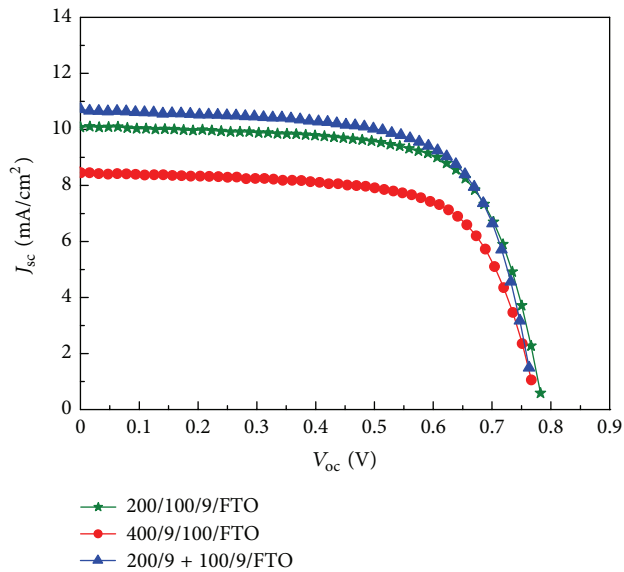


FIGURE 11: The photocurrent-voltage curves of DSSCs prepared by triple-layers with different particle sizes and the mixing of particle size in TiO_2 layers.

TABLE 6: The parameters of charge transfer resistance in triple-layer structures by EIS measurements.

Triple layers (nm)	R_s (Ω)	R_1 (Ω)	R_2 (Ω)
200/100/10/FTO	13.28	14.65	12.01
400/100/10/FTO	18.77	15.76	11.71
400/200/10/FTO	14.64	13.03	10.01

depends on the particle sizes of TiO_2 . The larger the particle sizes of TiO_2 , the shorter the optimal TiO_2 thickness. For double layers, the DSSCs with larger particle sizes in the top layer and smaller particle sizes in the bottom layer can obtain

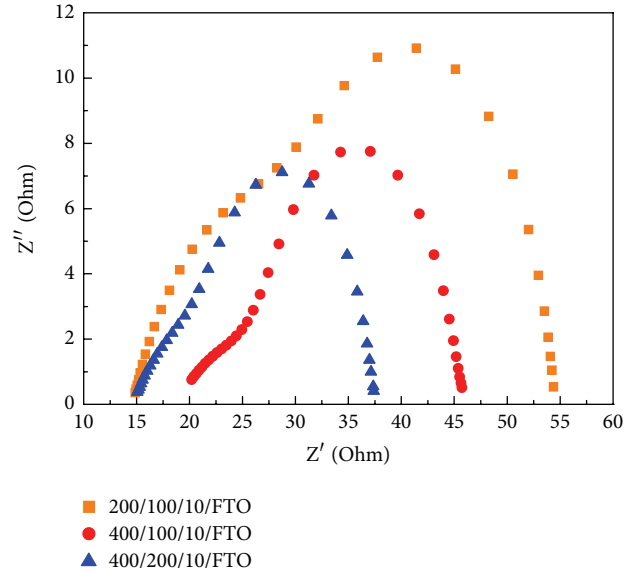


FIGURE 12: The EIS curves of DSSCs with the triple layer structures with different particle sizes of TiO_2 layers.

higher solar efficiency due to stronger back-scattering light and large surface area, respectively. The experimental results indicate that the choice of particle size in the bottom layer is more important than that in the top layer for achieving higher solar efficiency. For triple layers, the DSSCs with larger particle sizes in the top layer and smaller particle sizes on the bottom layer can also obtain higher solar efficiency. However, the choice of the particle sizes in the middle layer will depend on the particle sizes in the bottom and top layers. The mixing of the particle sizes in the middle layer is a good choice for achieving higher solar efficiency.

Acknowledgment

This work was supported by the National Science Council of Taiwan (Project no. NSC100-2221-E-182-037).

References

- [1] B. O'Regan and M. Gratzel, "A low-cost, high-efficiency solar cell based on dye-sensitized colloidal TiO_2 films," *Nature*, vol. 353, pp. 737–740, 1991.
- [2] M. Gratzel, "Conversion of sunlight to electric power by nanocrystalline dye-sensitized solar cells," *Journal of Photochemistry and Photobiology A*, vol. 164, pp. 3–14, 2004.
- [3] Q. F. Zhang, C. S. Dandeneau, X. Y. Zhou, and G. Z. Cao, "ZnO nanostructures for dye-sensitized solar cells," *Advanced Materials*, vol. 21, pp. 4087–4108, 2009.
- [4] S. Ito, T. N. Murakami, P. Comte et al., "Fabrication of thin film dye sensitized solar cells with solar to electric power conversion efficiency over 10%," *Thin Solid Films*, vol. 516, no. 14, pp. 4613–4619, 2008.
- [5] D. B. Kuang, S. Ito, B. Wenger et al., "High molar extinction coefficient heteroleptic ruthenium complexes for thin film dye-sensitized solar cells," *Journal of the American Chemical Society*, vol. 128, no. 12, pp. 4146–4154, 2006.

- [6] Q. F. Zhang and G. Z. Cao, "Nanostructured photoelectrodes for dye-sensitized solar cells," *Nano Today*, vol. 6, no. 1, pp. 91–109, 2011.
- [7] Y. Aswani, H. W. Lee, H. N. Tsao et al., "Porphyrin-sensitized solar cells with cobalt (II/III)-based redox electrolyte exceed 12 percent efficiency," *Science*, vol. 334, pp. 629–634, 2011.
- [8] Q. F. Zhang and G. Z. Cao, "Nanostructured photoelectrodes for dye-sensitized solar cells," *Nano Today*, vol. 6, no. 1, pp. 91–109, 2011.
- [9] J. S. Im, S. K. Lee, and Y. S. Lee, "Cocktail effect of Fe_2O_3 and TiO_2 semiconductors for a high performance dye-sensitized solar cell," *Applied Surface Science*, vol. 257, no. 6, pp. 2164–2169, 2011.
- [10] J. Ferber and J. Luther, "Computer simulations of light scattering and absorption in dye-sensitized solar cells," *Solar Energy Materials and Solar Cells*, vol. 54, no. 1–4, pp. 265–275, 1998.
- [11] G. Rothenberger, P. Comte, and M. Grätzel, "A contribution to the optical design of dye-sensitized nanocrystalline solar cells," *Solar Energy Materials and Solar Cells*, vol. 58, pp. 321–336, 1999.
- [12] M. Wei, Y. Konishi, H. Zhou, M. Yanagida, H. Sugihara, and H. Arakawa, "Highly efficient dye-sensitized solar cells composed of mesoporous titanium dioxide," *Journal of Materials Chemistry*, vol. 16, no. 13, pp. 1287–1293, 2006.
- [13] W. G. Yang, F. R. Wan, Q. W. Chen, J. J. Li, and D. S. Xu, "Controlling synthesis of well-crystallized mesoporous TiO_2 microspheres with ultrahigh surface area for high-performance dye-sensitized solar cells," *Journal of Materials Chemistry*, vol. 20, no. 14, pp. 2870–2876, 2010.
- [14] K. Yan, Y. Qiu, W. Chen, M. Zhang, and S. Yang, "A double layered photoanode made of highly crystalline TiO_2 nanooctahedra and agglutinated mesoporous TiO_2 microspheres for high efficiency dye sensitized solar cells," *Energy and Environmental Science*, vol. 4, no. 6, pp. 2168–2176, 2011.
- [15] D. H. Chen, F. Z. Huang, Y. B. Cheng, and R. A. Caruso, "Mesoporous anatase TiO_2 beads with high surface areas and controllable pore sizes: a superior candidate for high-performance dye-sensitized solar cells," *Advanced Materials*, vol. 21, no. 21, pp. 2206–2210, 2009.
- [16] Y. J. Kim, M. H. Lee, H. J. Kim et al., "Formation of highly efficient dye-sensitized solar cells by hierarchical pore generation with nanoporous TiO_2 spheres," *Advanced Materials*, vol. 21, no. 36, pp. 3618–3673, 2009.
- [17] I. G. Yu, Y. J. Kim, H. J. Kim, C. Lee, and W. I. Lee, "Size-dependent light-scattering effects of nanoporous TiO_2 spheres in dye-sensitized solar cells," *Journal of Materials Chemistry*, vol. 21, no. 2, pp. 532–538, 2011.
- [18] F. Sauvage, D. Chen, P. Comte et al., "Dye-sensitized solar cells employing a single film of mesoporous TiO_2 beads achieve power conversion efficiencies over 10%," *ACS Nano*, vol. 4, no. 8, pp. 4420–4425, 2010.
- [19] Y. C. Park, Y. J. Chang, B. G. Kum et al., "Size-tunable mesoporous spherical TiO_2 as a scattering overlayer in high-performance dye-sensitized solar cells," *Journal of Materials Chemistry*, vol. 21, no. 26, pp. 9582–9586, 2011.
- [20] M. J. Ross and K. R. William, *Impedance Spectroscopy: Emphasizing Solid Materials and Systems*, John Wiley & Sons, New York, NY, USA, 1987.
- [21] A. Hauch and A. Georg, "Diffusion in the electrolyte and charge-transfer reaction at the platinum electrode in dye-sensitized solar cells," *Electrochimica Acta*, vol. 46, no. 22, pp. 3457–3466, 2001.
- [22] Q. Wang, J. E. Moser, and M. Grätzel, "Electrochemical impedance spectroscopic analysis of dye-sensitized solar cells," *The Journal of Physical Chemistry B*, vol. 109, pp. 14945–14953, 2005.
- [23] N. Papageorgiou, W. F. Maier, and M. Grätzel, "An iodine/triiodide reduction electrocatalyst for aqueous and organic media," *Journal of the Electrochemical Society*, vol. 144, no. 3, pp. 876–884, 1997.
- [24] J. Bisquert, "Theory of the impedance of electron diffusion and recombination in a thin layer," *Journal of Physical Chemistry B*, vol. 106, no. 2, pp. 325–333, 2002.
- [25] K. Kalyanasundaram and M. Grätzel, "Applications of functionalized transition metal complexes in photonic and optoelectronic devices," *Coordination Chemistry Reviews*, vol. 177, pp. 347–414, 1998.
- [26] N. Koide, A. Islam, Y. Chiba, and L. Han, "Improvement of efficiency of dye-sensitized solar cells based on analysis of equivalent circuit," *Journal of Photochemistry and Photobiology A*, vol. 182, no. 3, pp. 296–305, 2006.
- [27] L. Han, N. Koide, Y. Chiba, and T. Mitate, "Modeling of an equivalent circuit for dye-sensitized solar cells," *Applied Physics Letters*, vol. 84, no. 13, pp. 2433–2435, 2004.
- [28] D. Qian, Y. Li, Q. Zhang, G. Shi, and H. Wang, "Anatase TiO_2 sols derived from peroxotitanium acid and to form transparent TiO_2 compact film for dye-sensitized solar cells," *Journal of Alloys and Compounds*, vol. 509, pp. 10121–10126, 2011.